Groundwater

In-Well Degassing of Monitoring Wells Completed in Gas-Charged Aquifers

by Tiago A. Morais[1,2] and M. Cathryn Ryan[2]

Abstract

Total dissolved gas pressure (P_{TDG}) measurements are useful to measure accurate in situ dissolved gas concentrations in groundwater, but challenged by in-well degassing. Although in-well degassing has been widely observed, its cause(s) are not clear. We investigated the mechanism(s) by which gas-charged groundwater in a recently pumped well becomes degassed. Vertical P_{TDG} and dissolved gas concentration profiles were monitored in the standing water column (SWC) of a groundwater well screened in a gas-charged aquifer for 7 days before and 15 days after pumping. Prior to pumping, P_{TDG} values remained relatively constant and below calculated bubbling pressure (P_{BUB}) at all depths. In contrast, significant increases in P_{TDG} were observed at all depths after pumping was initiated, as fresh groundwater with elevated in situ P_{TDG} values was pumped through the well screen. After pumping ceased, P_{TDG} values decreased to below P_{BUB} at all depths over the 15-day post-pumping period, indicating well degassing was active over this time frame. Vertical profiles of estimated dissolved gas concentrations before and after pumping provided insight into the mechanism(s) by which in-well degassing occurred in the SWC. During both monitoring periods, downward mixing of dominant atmospheric and/or tracer gases, and upwards mixing of dominant groundwater gases were observed in the SWC. The key mechanisms responsible for in-well degassing were (i) bubble exsolution when P_{TDG} exceeded P_{BUB} as gas-charged well water moves upwards in the SWC during recovery (i.e., hydraulic gradient driven convection), (ii) microadvection caused by the upward migration of bubbles under buoyancy, and (iii) long-term, thermally driven vertical convection.

Introduction

Monitoring of dissolved gases in shallow groundwater is important for a variety of applications in hydrogeological studies, such as determine groundwater residence times and flow paths (Wilson and Mackay 1995; Clark et al. 2004), analyzing subsurface biochemical reactions (Blicher-Mathiesen et al. 1998; Ryan et al. 2000), detecting the presence of free-phase gas (FPG) in the saturated zone (Manning et al. 2003; Amos et al. 2005; Solomon et al. 2011), and more recently, monitoring the occurrence of fugitive natural gas migration from oil and gas development (Jackson et al. 2013; Cahill et al. 2017; Forde et al. 2019; Roy et al. 2022) and carbon capture and storage sites (Boot-Handford et al. 2014; Lindeberg et al. 2017).

Increasing concerns associated with the expansion of unconventional O&G development have prompted research into long-term monitoring of unintended migration on natural gases from deeper zones into shallow groundwater (Jackson et al. 2013; Humez et al. 2016; Cahill et al. 2017; Bordeleau et al. 2021; Li et al. 2021), which can potentially have negative groundwater quality impacts and increase the risk of asphyxiation and explosion (Kelly et al. 1985; Jackson et al. 2013; Vengosh et al. 2014; Hammond 2016). The expansion of carbon capture, utilization, and storage studies (CCUS) has also increased the need for long-term monitoring of fugitive gases in the subsurface (Boot-Handford et al. 2014; Lindeberg et al. 2017). Thus, accurate long-term monitoring of total dissolved gas pressure (Roy et al. 2022) and dissolved gases concentrations (Humez et al. 2016; Campbell et al. 2022) in shallow groundwater is valuable in hydrogeological studies.

The accurate sampling and analysis of dissolved gas concentrations are particularly challenging in "gas-charged" or "gassy" aquifers (i.e., where in situ total dissolved gas pressure is elevated) because these wells are subject to *in-well* degassing when the water table

[1]Corresponding author: Tiago A. Morais, Geoscience, Univ. of Calgary, 2500 University Drive NW, Calgary, Alberta, Canada; +1 (587) 429 2407; tamorais@ucalgary.ca

[2]Department of Geoscience, University of Calgary, Calgary, Alberta, Canada; cryan@ucalgary.ca

Article impact statement: Dissolved groundwater gas concentrations are subject to in-well degassing in gas-charged groundwater wells in the absence of pumping.

Received April 2022, accepted July 2022.

doi: 10.1111/gwat.13238

is lowered due to pumping during sampling (Roy and Ryan 2010; Roy and Ryan 2013). An increasing number of studies have demonstrated that the use of total dissolved gas pressure (P_{TDG}) sensors (Manning et al. 2003; Roy and Ryan 2010, 2013; Roy et al. 2022) combined with passive gas diffusion samplers (PGDs) or downhole samplers can provide a better analytical resolution when estimating in situ gas concentrations in gas-charged aquifers (Spalding and Watson 2006, 2008; McLeish et al. 2007; Banks et al. 2017; Evans 2017). Passive gas diffusion samplers (PGDs) consist of a gas void volume adjacent to a gas permeable water barrier (e.g., silicone), which allows dissolved gases in the aqueous phase to equilibrate within the gas void volume after an appropriate amount of time (McLeish et al. 2007), providing a sample of equilibrated gas species composition. After deployment, gas samples are recovered and isolated for storage before injection into a gas chromatograph to measure the relative composition of each gas species of interest at ambient laboratory pressure.

The solubility of a given gas in liquid can be described according to Henry's law, which states that the concentration of a gas species dissolved in liquid (C_i) is proportional to its partial pressure (P_i) above the liquid (Equation 1; where H_i is the Henry's law constant for a gas species i as function of temperature and salinity). Furthermore, according to Dalton's law of partial pressures, P_{TDG} is equal to the sum of the partial pressures of all the gases dissolved in the liquid (ΣP_i) and the water vapor pressure (P_{WV}) (Equation 2). Since the amount of gas dissolved in liquid is proportional to its partial pressure, the concentration of each gas species (i) in situ can be calculated from the combined measurement of in situ P_{TDG} and relative gas composition measured in the laboratory (McLeish et al. 2007; Roy and Ryan 2010).

$$H_i\ (T, S) = \frac{C_i}{P_i} \tag{1}$$

$$P_{TDG} = \Sigma P_i + P_{WV} \tag{2}$$

Field hydrogeologists often measure water levels using downhole pressure transducers that measure "total pressure," or the sum of atmospheric and water pressures. In this context, P_{TDG} is often expressed as total pressure (e.g., Roy and Ryan 2010; i.e., equal to atmospheric pressure at the water table). This offers the advantage of P_{TDG} being consistent with the sum of partial pressures for all gas species present (P_i in Equation 2) in the correct form (i.e., where it is equal to P_{ATM} at the water table). In order to compare the downhole pressure directly, in this manuscript, unless otherwise noted, P_W values refer to "total water pressure" which includes atmospheric pressure (as do P_{TDG} and P_{BUB} values).

The field estimation of in situ P_{TDG} overcomes the major challenge inherent in sampling and analysis of gassy groundwater, namely the loss of gas species from groundwater samples by degassing (i.e., formation of free-phase gas or bubbles), which is can also be observed in unpumped groundwater wells under natural conditions (Waddington et al. 2009; Roy and Ryan 2010), and is notably induced by well pumping (Roy and Ryan 2010). The formation of free-phase gas, or bubbles, can strip gases from groundwater during pumping, lowering the P_{TDG} and reducing the accuracy of the measured gas concentrations relative to in situ concentrations (Ryan et al. 2015). In standing water columns, free phase gas will travel upwards under buoyancy and be lost from the water column (Lu et al. 2005; Waddington et al. 2009; Watson et al. 2014). Free phase gas (or bubble) formation is initiated when P_{TDG} is equal to bubbling pressure (P_{BUB}), where P_{BUB} is equal to the sum of total water pressure (P_W) and capillary pressure (P_{CAP}) at a given point (Equation 3; Manning et al. 2003; Roy and Ryan 2013).

$$P_{BUB} = P_W + P_{CAP} \tag{3}$$

In gas-charged wells that have not been pumped recently, measured P_{TDG} is consistently lower than P_{BUB} in the standing water column (SWC), and often observed to increase to P_{BUB} conditions when the well is pumped without significant lowering of the water table (i.e., without significantly lowering P_W and P_{BUB} during pumping; Roy and Ryan 2010; Evans 2017; Banks et al. 2017). The occurrence of P_{TDG} that is consistently less than P_{BUB} in unpumped wells screened in gas-charged aquifers suggest degassing occurs in the SWC, likely by some process that causes in-well mixing (Roy and Ryan 2010; Evans 2017). Although in-well degassing in gas-charged wells has been implied in the literature, to our knowledge, it has not been clearly demonstrated nor has its cause(s) been systematically investigated. Since measuring P_{TDG} is important to obtain accurate in situ dissolved gas concentrations, it is similarly important to understand the mechanisms and rate by which P_{TDG} in gas-charged groundwater wells decrease after pumping ceases, and the degree to which in-well degassing occurs to facilitate accurate in situ P_{TDG} measurements.

In-well mixing can occur for several reasons in groundwater monitoring wells, including hydraulic gradient-driven advection (particularly in wells with long screens) and advective flows driven by density and/or temperature gradients in the SWC (Barczewski et al. 1993; Solodov et al. 2002; Berthold and Börner 2008). Furthermore, the buoyant migration of FPG (i.e., rise of bubbles) in vertical water columns can induce solute mixing by inducing turbulence without mechanical agitation in industrial applications (Climent and Magnaudet 1999; Almeras et al. 2015). Further, turbulence-induced convection increases in strength as bubbles increase in size (due to decreasing P_W) during their buoyant ascent. The end result is movement of deeper water (i.e., gas-charged) to the top of the SWC (i.e., vertical mixing) and shallow water towards the bottom of the SWC. Although multiple drivers of in-well mixing in groundwater monitoring wells have been implied and observed, there is no field study that demonstrates if in-well mixing can also induce degassing in groundwater wells screened in gas-charged aquifers.

Therefore, the main objective of this study was to collect field data from the SWC of gas-charged wells to demonstrate the occurrence of in-well degassing and gain insight into the process(es) by which groundwater in wells becomes mixed and degassed. The mechanism and rates of degassing processes were investigated by measuring P_{TDG} at multiple depths in the SWC of a groundwater monitoring well before and after groundwater pumping. Passive gas diffusion samples were also collected to determine changes in gas composition with depth in the well water column. Finally, sulfur hexafluoride (SF_6) gas tracer was added into the top of the 41 m high water column and throughout the well casing headspace above the SWC immediately after pumping, and its concentration in the water column measured after 15 days to evaluate the occurrence of in-well mixing (in tandem with changes in concentration of the major gas species derived from the atmosphere and/or groundwater).

Site Description

This study was conducted in an Alberta Environment groundwater monitoring well located in the town of Rosebud, Alberta (Rosebud #2: GOWN ID: 0972; Blyth and Mellor 2009). Previous water well testing in the area showed elevated biogenic CH_4 concentrations in shallow aquifers containing coals and shales (Humez et al. 2016). The 125 mm (4.94-in.) diameter Rosebud #2 monitoring well is completed in the Horseshoe Canyon Formation at a total depth of 55.5 m below ground surface (bgs), with a screened interval between 52.5 and 55.5 m bgs that crosses layers of sandstone, shale, and a water bearing coal zone (Blyth and Mellor 2009). The average static water level for this during the field work campaigns was approximately 14.5 m bgs, leading to a static water column height of about 38.0 m above the top of the screen (Figure 1).

Previous studies have shown that in situ groundwater volumetric gas composition in Rosebud #2 is ~89.3% CH_4, 9.0% N_2, 1.5% O_2 and 0.2% CO_2, with an average in situ total P_{TDG} (i.e., including atmospheric pressure) of ~403 KPa (Castellon 2009; Roy and Ryan 2010; Evans 2017). Given the local P_{ATM} of ~92 kPa, the in situ gauge P_{TDG} (311 kPa) is equivalent to about 31.7 m freshwater head in the well's SWC. Given the SWC is 38.0 m at the top of the screen, the aquifer is undersaturated with respect to P_{TDG} (i.e., at about 83% of its P_{BUB} at the top of the screen). Thus, if the study well were (i) recently pumped, (ii) recovered to static level, and (iii) degassed only to P_{BUB} at any given depth (i.e., no in-well degassing), then the vertical distribution of P_{TDG} in the SWC would be expected to equal to P_{BUB} until the value of P_{BUB} reaches the aquifer P_{TDG} measured in this study, which occurs at $P_{BUB} = 396.2$ kPa (absolute), or ~31.0 m bswl. Below this depth, the P_{TDG} would remain at the aquifer value. For the purposes of this article, we define this vertical distribution (shown as a red line in Figure 2) as the "equilibrium" P_{TDG} for the Rosebud #2 well that would exist in the absence of in-well mixing.

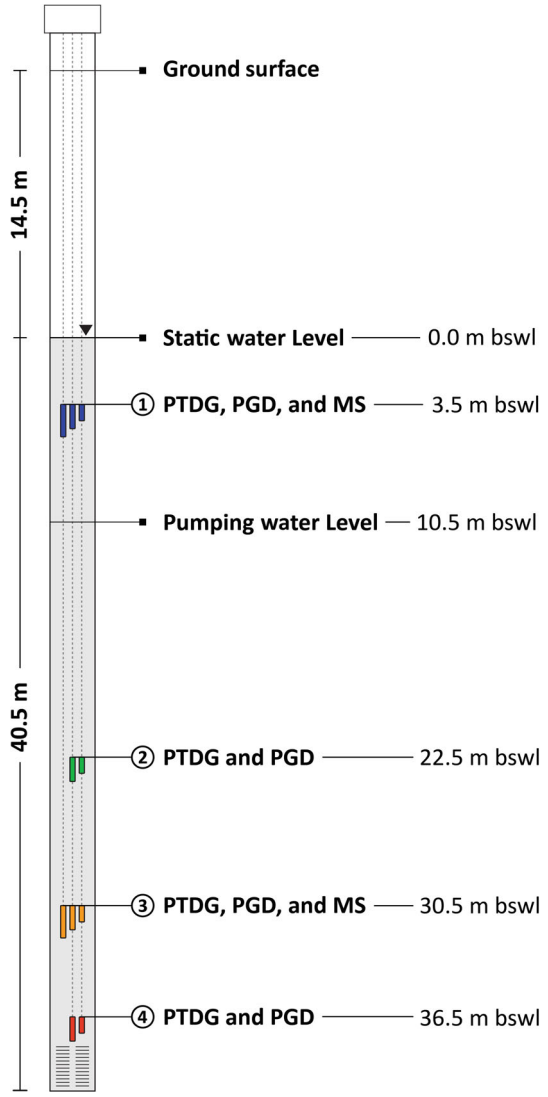

Figure 1. Schematic figure of groundwater instrumentation installed at Rosebud #2 (GOWN ID: 0972), including the instrumentation deployed at four monitoring depths (3.5, 22.5, 30.5, and 36.5 m bswl), the static water level, and the water level maintained during well pumping. The equipment deployed at each depth is labeled as follows: P_{TDG} is the total dissolved gas pressure probes, PGD is the passive gas diffusion sampler; MS is the multilevel sondes (which measured water pressure, dissolved oxygen, and temperature).

Materials and Methods

Two consecutive fieldwork campaigns (denoted pre- and post-pumping) were separated chronologically by groundwater pumping from the groundwater monitoring well as described below. During both monitoring periods, custom-made P_{TDG} sensors (Roy and Ryan 2013) and passive gas diffusion samplers (McLeish et al. 2007) were deployed at four monitoring depths (3.5, 22.5, 30.5, and 36.5 m below the static water level [bswl]; Figure 1). Two multiparameter minisondes (Hydrolab MS5, Hatch®) were also deployed at 3.5 and 30.5 m bswl to measured water level (±0.05 m), dissolved O_2 (±0.1 mg/L), and temperature (±0.1°C) within the well water column.

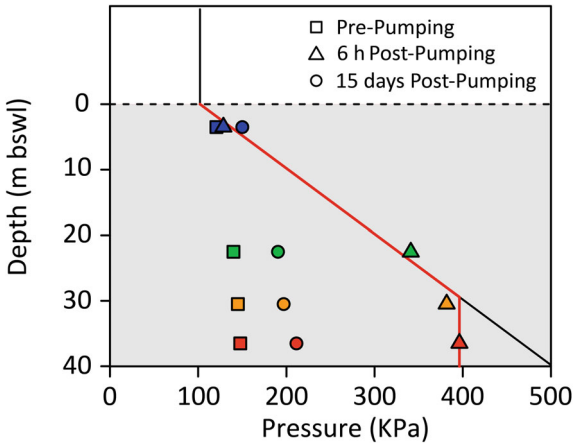

Figure 2. Measured P_{TDG} with depth (i) when monitoring equipment was recovered after the pre-pumping monitoring period (squares), (ii) ~6 h post-pumping (i.e., when maximum P_{TDG} values were observed; triangles), and (iii) when the post-pumping monitoring equipment was recovered (i.e., 15 days after pumping; circles). The solid black line shows equal P_{TDG} and P_{BUB} and the red line shows the expected P_{TDG} profile for the study well, which is limited by the measured aquifer value of P_{TDG} of 396.2 kPa in the screened interval (38.0–41.0 m bswl). The red line corresponds to either P_{BUB} or the aquifer P_{TDG} at the screen (whichever is less; Table 2). The symbol colors correspond to sampling depths (c.f. Figure 1).

The minisondes were calibrated in the field immediately before each deployment and programmed to take hourly measurements. A summary of the dates of equipment deployment and recovery are shown in Table 1.

Sulfur hexafluoride, a stable gas species that is not affected by most chemical and biochemical processes (Watson et al. 1991), has been extensively used as tracer in hydrogeology studies (Wilson and Mackay 1993; Wilson and Mackay 1995; Harden et al. 2003). Atmospheric background concentrations of SF_6 are between 1 and 2 parts per trillion by volume (Watson et al. 1991), and essentially zero in background natural groundwater systems (Wilson and Mackay 1993). Therefore, SF_6 was used as a tracer to provide further insight into the occurrence and rate of in-well mixing during the post-pumping monitoring period.

Pre-Pumping Monitoring

The minisondes, P_{TDG} sensors, and passive gas diffusion samplers were deployed as described above for a period of 7 days before retrieval (at which point the monitoring well had not been pumped for more 64 days beforehand). Throughout this monitoring period, small drill holes above grade in the well casing ensured there was no difference between the gas pressure in the well casing headspace and atmospheric pressure.

Groundwater Pumping and Post-Pumping Monitoring

The post-monitoring period was preceded by pumping of approximately 450 L over several hours to bring fresh groundwater with in situ P_{TDG} into the well casing. The total volume pumped was equivalent to ~1.1 times the volume of the SWC at static level, or ~1.4 times the SWC while pumping. An electrical pump (Waterra Hydrolift®) connected to a 0.625-in. HDPE tubing and a 1-in. OD foot valve (Waterra D-25®) was positioned 10.5 m bswl (Figure 1). The foot valve only pumps effectively when the water level was at least 10.5 m below static (or 25 m bgs), ensuring that "fresh" or aquifer groundwater with elevated P_{TDG} would be present at all monitoring depths shortly after ending of pumping.

Immediately after pumping ceased, the well water level was 10.5 m bswl, and P_{TDG} sensors, minisondes, and passive gas diffusion samplers were re-deployed within 10 min, as described above. Shortly after the re-deployment of all the equipment, ~12.5 L of SF_6 were bubbled into the well water column, about 0.25 m below the water level over a short period (i.e., ~2 min). An additional 250 L of SF_6 was subsequently also pumped into the well casing ~2.0 m above the measured water level over a period of ~10 min. The SF_6 tracer was introduced to the well via a 12.7 mm diameter polyethylene tubing attached to the regulator of a compressed gas cylinder. As the molecular weight of SF_6 is substantially heavier (146 g/mol) than any of the dominant gas species present in the well casing derived either from the atmosphere

Table 1
Summary of the Field Activities Conducted in the Rosebud #2 (GOWN ID: 0972) Groundwater Monitoring Well During the Two Consecutive Fieldwork Campaigns

	Pre-Pumping		Post-Pumping		
Equipment	**Jan 31**	**Feb 7**	**Feb 17**	**Mar 4**	**Setup/Configuration**
P_{TDG} sensors	Deployed	Collected	Deployed	Collected	Probes installed at four different depths to measure P_{TDG} every 30 min
PGD's	Deployed	Collected	Deployed	Collected	Passive gas diffusion samplers installed at four different depths
Minisondes	Deployed	Collected	Deployed	Collected	Minisondes installed at four different depths
Duration of pumping	—	—	3 h[a]	—	Approximately 450 L pumped at a rate of ~20 L/min[a]

[a] Intermittent pumping.

(i.e., N_2 or O_2, with molecular weights of 28 and 32 g/mol, respectively), or groundwater (i.e., CH_4, N_2, or CO_2, with molecular weights of 16, 28, and 15 g/mol, respectively), the SF_6 would have displaced any pre-existing gas species in the well casing headspace from the bottom to the top as the SF_6 was injected. After the injection of SF_6, the well casing was sealed with duct tape, leaving the upper surface of the well water column free to interact with SF_6 and reasonably isolated from advective exchange with the atmosphere for the duration of the post-pumping monitoring period. Due to the multiple cables that needed to be accommodated at the wellhead so that downhole probes could be attached to external data loggers, the wellhead was wrapped with duct tape to prevent advective exchange with the atmosphere. Fifteen days after deployment, P_{TDG} sensors, minsondes, and passive gas diffusion samplers were retrieved to recover the post-pumping data.

P_{TDG} Measurements

In-well P_{TDG} profiles were measured using commercial SDX100A4 pressure sensors (Honeywell®) connected to a gas-permeable silicone tubing (0.38 mm ID and 0.79 mm OD) constructed as described in previous studies (Manning et al. 2003; Roy and Ryan 2013). The pressure transducers were soldered onto cables, sealed with epoxy, and then connected to a CR100 data logger (Campbell Scientific®), which was programmed to measure P_{TDG} values every 30 min during both monitoring periods. P_{TDG} sensors were laboratory-calibrated prior to deployment by recording the output signal in an enclosed vessel filled with air and containing all sensors at a variety of known gas pressures that were set using a gas regulator fitted on a compressed air cylinder. The equilibration time for dissolved gases to diffuse across the silicon membrane and reach equilibrium depends on the surface area to volume ratio, gas permeability, and thickness of the silicon tubing (Manning et al. 2003; D'Aoust 2007). Based on unpublished data, the equilibration time for the P_{TDG} sensors used is approximately 20 min with an accuracy of ±5.0%. Variations in the battery charge (which was charged by a solar panel at a rate affected by incoming solar radiation) affected the voltage sent downhole to the custom-made P_{TDG} sensors by the datalogger, and hence to the logged P_{TDG}. Thus, raw P_{TDG} data was corrected for the actual measured voltage using an empirically determined equation (see Equation S1).

Dissolved Gas Sampling and Analysis

Dissolved gas concentrations were estimated by combining gas composition from passive gas diffusion samplers (Sanford et al. 1996; McLeish et al. 2007) and measured P_{TDG} (Roy and Ryan 2013). In this study, duplicate 1 mL gas-tight syringes (Vici®) press fit onto a 75 mm long silicone tubing (OD: 6 mm; ID: 4 mm) were deployed at all monitoring depths. Passive gas diffusion samplers were collected at the same time that the P_{TDG} and minisonde probes were recovered after each of the pre- and post-pumping period (Table 1). While pre-pumping gas samples were collected 7 days after the first deployment, post-pumping gas samples were collected 15 days after the second deployment. Immediately after retrieval, the syringe stopcock valve was pushed into the closed position, isolating the sample for storage (submerged in well water) prior to gas chromatography analysis, which occurred within 2 days of sample retrieval.

Passive gas diffusion samples were directly injected into a HP-5890 (Hewlett-Packard®) gas chromatograph via a six-port, two-position sample valve with a 5 μL sample loop that was manually loaded from the dissolved gas sampler (McLeish et al. 2007). The gas chromatograph was equipped with a D-1 pulse discharger (Valco®) and two parallel columns (Rt-Msieve 5A Restek, 30 m × 0.32 mm and Rt-Q-PLOT Restek, 30 m × 0.53 mm) to estimate CH_4, SF_6, CO_2, Ar, O_2, and N_2 volumetric compositions. While the sampling valve, injection line, and gas chromatograph oven were maintained at a constant temperature of ~30°C, the detector was held at ~200°C. Prior to each analysis, a certified gas standard (5.0% CH_4, 5.0% CO_2, 5.0% N_2, 4.5% O_2, and 1.0% Ar) and dilutions of pure N_2, SF_6, and CH_4 gases with He as a diluent were used to calibrate the gas chromatograph. Pure He (99.999%) was used as carrier gas. Analytical precision is typically better than ±1.0% of the reported values, and the reported lower detection limit ranges from 0.001% to 0.05% by volume depending on the gas species. Finally, an average gas composition at each depth was calculated for the pre- and post-pumping monitoring period based on the gas composition measured from the duplicate samples collected at each depth.

Dissolved Gas Concentration Estimates

Dissolved gas concentrations were estimated using Henry's Law and the P_{TDG} values recorded at the four monitoring depths when samples were collected. First, the volumetric composition of each gas (%vol) estimated by the gas composition analysis were converted into partial pressure (P_i) using the decimal equivalent and the correspondent in situ P_{TDG} value (P_{TDG}; Equation 4). Once the volumetric compositions were converted into partial pressures for each gas species, the aqueous concentration (C_i; mg/L) of each can be calculated multiplying the correspondent partial pressure (P_i) by the Henry's law constant for the appropriate in situ temperature and groundwater salinity (H_i), and the molecular weight of the gas of interest (MW_i; Equation 5). Henry's law Constants data were obtained from Sander (2015) and Busenberg and Plummer (2010).

$$P_i = \frac{\%\text{vol}}{100} P_{TDG} \quad (4)$$

$$C_i = P_i \, H_i \, MW_i \, 1000 \quad (5)$$

Dissolved gas concentrations at the beginning of the pre-pumping and at the end of the post-pumping monitoring periods were estimated based on the average gas compositions obtained at each depth for each monitoring period and their respective P_{TDG} values at the same depths at the

time of sample collection. Gas concentrations were also estimated when peak P_{TDG} values were measured 6 h after pumping ended (i.e., 6 h into the post-pumping monitoring period). In the absence of PGD samples, groundwater gas concentrations estimates were based on the measured post-pumping gas composition at each monitoring depth and measured P_{TDG} values at the same depths.

In-Well Mixing Driven by Hydraulic Gradient, Buoyant Bubble Transport, and Thermal Gradient

Three drivers of in-well mixing were considered, including well water flow induced by hydraulic gradient (which is well known to occur, and reflected by a rising water level during recovery from pumping), buoyant transport of bubbles, and thermal gradient-induced mixing.

As FPG formation is only expected to occur in the SWC when P_{TDG} exceeds P_{BUB}, the FPG formation and rise in the SWC (under buoyancy) was assumed to occur whenever measured P_{TDG} exceed P_{BUB} over the monitoring period at each of the four deployment depths (Figure 1). In contrast, the induction of in-well water flow was evaluated by considering the change in pressure at the two depths where water pressure was measured (3.5 and 30.5 m bswl; Figure 1). Finally, the occurrence of thermally induced convection was investigated by using temperature measurements at 3.5 and 30.5 m bswl to conduct thermal stability analysis over the monitoring period.

Rayleigh's theory is commonly used to conduct thermal stability analyses and evaluate the potential for the occurrence of thermally driven convection (or mixing) in boreholes and groundwater wells (Solodov et al. 2002; Love et al. 2007; Berthold and Börner 2008; Berthold 2010). Thermally driven convection occurs in vertical water columns when the thermal Rayleigh number (Ra_T) exceeds the critical thermal Rayleigh number (Ra_{TC}; Rayleigh 1916), where a dimensionless Rayleigh number for thermal driven convection Ra_T can be determined as:

$$Ra_T = \frac{ge(\Delta T)r^4}{hvd} \tag{6}$$

where g is the gravity acceleration ($m\,s^{-2}$), e is the thermal expansion coefficient of water ($^{\circ}K^{-1}$), ΔT is the temperature gradient within the well water column ($^{\circ}K$), r radius of the well water column (m), h is the height of the water column (m), v is the kinematic viscosity of water ($m^2\ s^{-1}$), and d is the thermal diffusivity of water ($m^2\ s^{-1}$).

For large diameters wells ($h \gg$ radius) the critical thermal Rayleigh number can be estimated using the following approximation (Gershuni and Zhukhovitskii 1976):

$$Ra_{TC} = \frac{96}{5(1+7\lambda)}\left[3(33+103\lambda) - \sqrt{3(2567+14{,}794\lambda+26{,}927\lambda^2)}\right] \tag{7}$$

where λ is the ratio of the thermal conductivities of the well water and surrounding material.

Thus, stability analysis using Rayleigh's theory was conducted to assess the occurrence of favorable conditions for the development of thermal convection. Given the characteristics of the RBD2 well ($h \gg$ radius), Equations 6 and 7 can be utilized to obtain Ra_T and Ra_{TC}. The hourly temperature measurements from the minisondes installed at 3.5 and 30.5 m bswl were used to calculate hourly Rayleigh numbers for thermal driven convection (Ra_T) over the 15-day post-pumping monitoring period and then compared with the critical thermal Rayleigh number (Ra_{TC}) to evaluate the likelihood of the occurrence of thermal induced convection within the well water column.

Results and Discussion

Field Parameters and Estimated Bubbling Pressure (P_{BUB})

The water level in the SWC recovered in a typical post-pumping "recovery" fashion from 10.5 m bswl to the previous static level over about 16 h (Figure S1). Temperature and dissolved O_2 remained relatively constant during the pre- and post-pumping period, suggesting that biochemical conditions in the SWC were similar during both monitoring periods (Table S1). Although dissolved O_2 fluctuations (i.e., between 0.0 and 2.1 mg/L) were observed during the pre-pumping period, dissolved O_2 values remained constantly below detection (<0.1 mg/L) during the post-pumping period. Since multisondes were not deployed at 22.5 and 36.5 m bswl (Figure 1), the P_{BUB} at these depths were interpolated from those recorded by the minisondes deployed at 3.5 and 30.5 m bswl. The bubbling pressure (P_{BUB}) at each monitoring depth was calculated as the sum of the atmospheric pressure (P_{ATM}; locally ~92 kPa) and measured hydrostatic pressure (P_W). The estimated P_{BUB} at the top of the screened section (38.0 m bswl) was 464.4 kPa when the water level was at static, and 366.3 kPa immediately after pumping was ceased (i.e., when the water level was ~10.5 m bswl). The P_{BUB} at each monitoring depth increased proportionally with the depth of sensor deployment (Figures 2 and 3; Table 2).

Pre-Pumping P_{TDG} Measurements

The P_{TDG} values remained relatively constant at all monitoring depths during the pre-pumping monitoring period (Figure 3A–3D). Although P_{TDG} values remained close to P_{BUB} at the shallowest monitoring point (35.0 m bswl), pre-pumping P_{TDG} values were consistently lower than the corresponding P_{BUB} (or equilibrium P_{TDG} for the 36.5 m bswl deployment depth) at all monitoring depths, but markedly so at 22.5, 30.5, and 36.5 m bswl (Table 2; Figure 3A–3D). The relatively low P_{TDG} values indicated that the unpumped SWC was undersaturated with respect to P_{BUB} and that P_{TDG} just above the screened interval (i.e., 36.5 m bswl) was significantly lower than the in situ aquifer P_{TDG} (403 KPa; Castellon 2009; Roy and

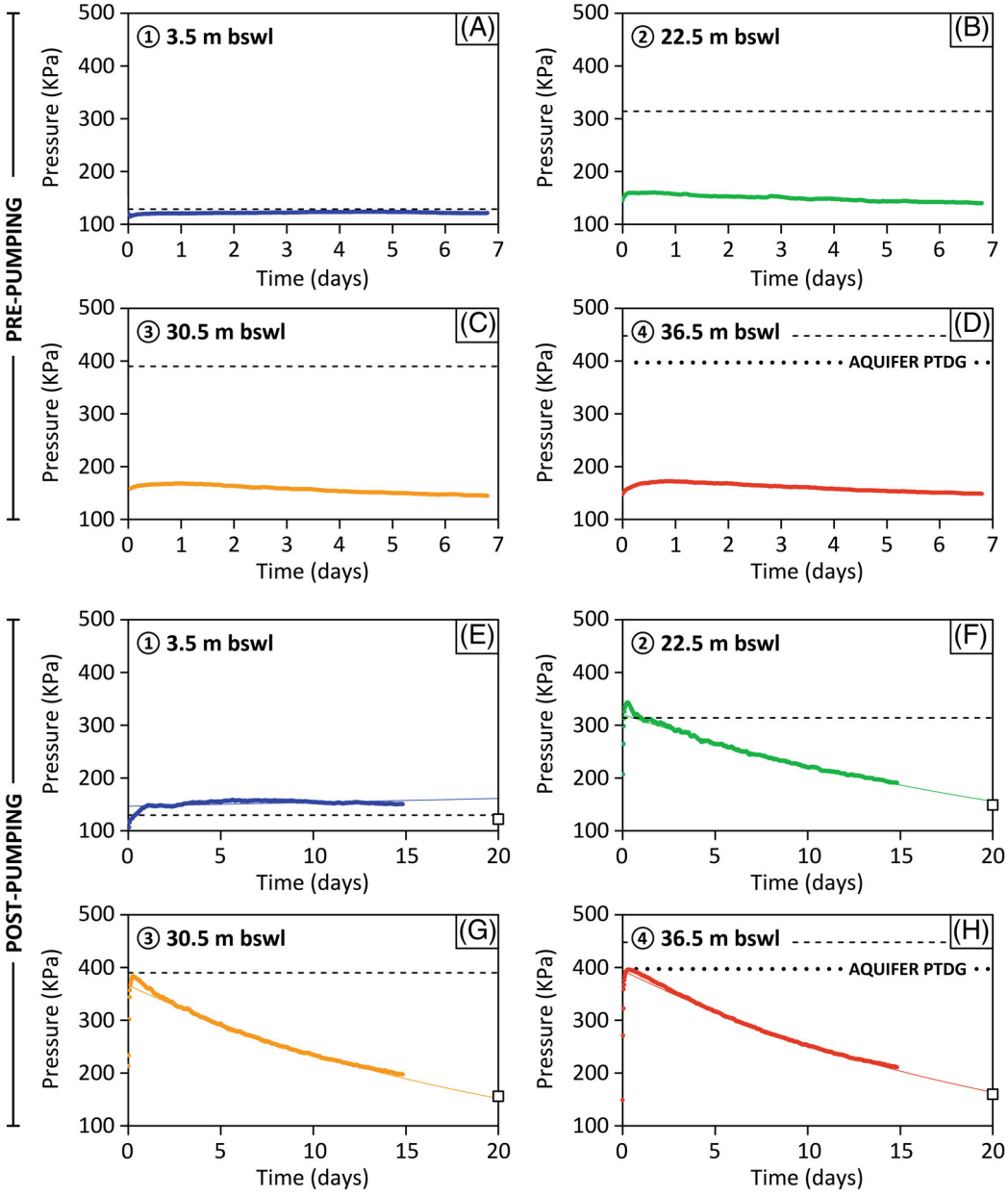

Figure 3. Times series of total P_{TDG} values during the pre- (A–D) and post-pumping (E–H) monitoring periods at 3.5, 20.5, 30.5, and 36.5 m bswl. Measured data are plotted as points and/or thicker lines, while best fit trendlines are shown as thin solid lines. The P_{BUB} values for each monitoring depth at static water level are shown as black dashed lines, and the "aquifer P_{TDG}" (i.e., 396.2 kPa total pressure) is shown as a dotted line for the 36.5 m bswl monitoring depth. Assumed P_{TDG} values after 20 days are taken as the average value of P_{TDG} at each monitoring depth prior to pumping (i.e., degassed water) and are shown as black empty squares.

Ryan 2010; Evans 2017). Values of P_{TDG} that were increasingly lower than P_{BUB} with depth confirmed that substantial in-well degassing caused P_{TDG} to decrease in the SWC after pumping (Figure 2; Table 2). The relatively stable P_{TDG} values observed at all depths over the pre-pumping monitoring period indicated that substantial degassing did not actively occur over the pre-pumping monitoring period (Figure 3A–3D). However, it is important to note that a P_{TDG} gradient with depth was also observed during the pre-pumping monitoring period, indicating the SWC was not completely degassed and there was still potential for the occurrence of gas species exchange between the SWC and the atmosphere 64 days after pumping (Figure 2; Table 2).

Since the P_{TDG} values remained lower than P_{BUB} over the pre-pumping period, bubbles formation was not likely, and, therefore, the SWC degassing (and mixing) was reduced throughout the pre-pumping monitoring period. As the deeper water column would have contained "fresh" groundwater with in situ P_{TDG} values representative of the aquifer water after the last pumping event (64 days), degassing of the SWC occurred prior to the pre-pumping monitoring period. Furthermore, the fact that the water column was also degassed at depths where P_{BUB}

Table 2
Bubbling, Total Dissolved Gas Pressure for No In-Well Degassing, and Total Dissolved Gas Pressures Measured at Four Monitoring Depths in Different Parts of Pre- and Post-Pumping Monitoring

Deployment Depth[a]						
m bswl	m bgs	P_{BUB} (kPa)	P_{TDG} for no in-well degassing[b] (kPa)	Average pre-pumping P_{TDG} (kPa)	Max P_{TDG} measured[c] (kPa)	Aquifer P_{TDG} at the screen (kPa)
3.5	18.0	126.3	126.3	122.1	140.3	
22.5	37.0	312.6	312.6	149.4	343.4	396.2
30.5	45.0	391.1	391.1	156.4	383.6	
36.5	51.0	450.0	396.2	160.4	396.2	

Note: All pressures are total (i.e., the sum of gauge and the local atmospheric pressure of about 92 kPa).
[a] As shown in Figure 1.
[b] As shown in Figure 2.
[c] Approximately 6 h post-pumping.

was greater than the in situ P_{TDG} (i.e., 3.5, 22.5, 30.5, and 36.5 m bswl; Figure 2) suggests that processes other than bubble-induced mixing might be contributing to in-well degassing, as bubbles are not expected to occur at depths where P_{TDG} is lower than P_{BUB}.

Post-Pumping P_{TDG} Measurements

During the first 6 h of post-pumping monitoring, water pressure and P_{TDG} values increased at all four monitoring depths (Figures 3E–3H and 4). This rise of P_{TDG} after the pump shut off is attributed to fresh groundwater with an in situ P_{TDG} entering the well and flowing upwards in the casing as the well water level gradually recovered to static (which concurrently increased the P_{BUB} at each point). Immediately after pump shut was off, the well water level was at 25.0 m bgs, with ~95% of the recovery (to 15.0 m bgs) occurring over 3 h, with recovery to static water level (14.5 m bgs) effectively complete about 16 h after pumping ceased (Figure 4B). The increasing water pressure over the first 16 h of recovery resulted in commensurate increases in P_{BUB} at all monitoring depths over the 16-h recovery period. The initial increasing P_{TDG} at all monitoring points thus reflected the combination of increased P_{TDG} in "fresh" groundwater as it moved up the well casing at the same time that P_{BUB} was increasing due to well recovery, balancing gas species mass loss ebullition (i.e., by bubble formation, upward transport under buoyancy and loss to the headspace in the well casing) over the same period. The combination of these processes caused the P_{TDG} values to reach their highest values (i.e., maximum P_{TDG}) approximately 6 h after end of pumping (Figure 4B).

The P_{TDG} at 36.5 m bswl (i.e., 1.5 m above well screen) was ~322 kPa shortly after pumping ceased, and continued to rise for approximately 6 h, at which time it reached the maximum value observed (~396.2 kPa; Table 2; Figures 3H and 4). Ebullition (bubble formation) was audible with the human ear during pumping and immediately after pump shut-off. The aquifer in situ P_{TDG} value was never reached in any other monitoring depth (Figures 2 and 3E–3H), which is consistent with active degassing by bubble formation. After the maximum P_{TDG} values were observed, P_{TDG} values decreased at all depths throughout the post-pumping monitoring period (Figure 4). The rate of degassing (as represented by the rate of decline in P_{TDG} values) declined exponentially over the 15-day monitoring period (Figure 4A). The P_{TDG} values did not reach their pre-pumping values after 15 days, suggesting degassing was still actively occurring at this time. The best fit extrapolation of the observed decline in P_{TDG} at each monitoring depth suggest the pre-pumping values would be reached ~20 days after pumping (Figures 3E–3H and 4A). As P_{TDG} at the two deepest monitoring depths remained below the "equilibrium" value (Figure 2) during the entire monitoring period and decreased over time (Figure 3E–3H), degassing must also have occurred at depths despite in situ P_{TDG} values that were lower than the respective "equilibrium" P_{TDG} values (shown as a red line in Figure 2).

During the first 16 h after pumping, the P_{TDG} was equal to P_{BUB} at 3.5 and 22.5 m bswl (Figures 3E and 3F), suggesting that active formation of bubbles occurred at these depths, with consequently active degassing of the well water column. The P_{TDG} at 22.5 m decreased to below P_{BUB} and remained that way for the rest of the monitoring period. In contrast, the P_{TDG} at the shallowest monitoring depth (3.5 m bswl) remained ~20 kPa above P_{BUB} during the entire post-pumping monitoring period, suggesting continuous favorable conditions to the formation of FPG within in this interval.

The higher rate of degassing during the first 16 h is consistent with the P_{TDG} measurements with depth, since more favorable conditions for bubble formation existed in the well water column (i.e., P_{TDG} > "equilibrium" P_{TDG}) compared with the rest of the monitoring period. The rate of degassing decreased exponentially over the post-pumping period as P_{TDG} values (and difference between P_{TDG} and "equilibrium" P_{TDG}) declined, along with the consequent tendency to form bubbles. By the end of the 15-day post-pumping monitoring period, P_{TDG} only exceeded P_{BUB} in the shallowest monitoring point (Figures 2 and 3E). P_{TDG} measurements did not stabilize at any of the four monitoring depths even after 15 days post-pumping, suggesting in-well degassing was ongoing (albeit at a decreased rate).

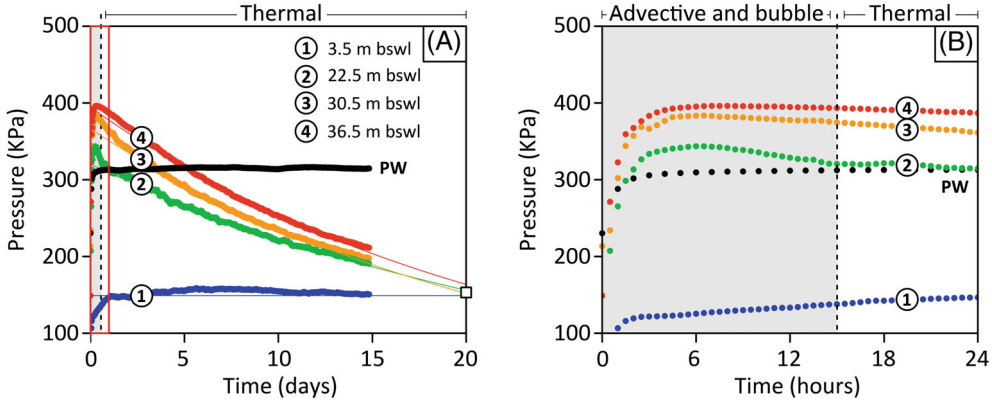

Figure 4. (A) Time series of water pressure (PW) and P_{TDG} values in the post-pumping monitoring period. The P_{TDG} was monitored at 3.5, 22.5, 30.5, and 36.5 m bswl. Best fit (exponential) extrapolations of measured P_{TDG} values at each monitoring depth are shown as thin solid lines, and the average measured P_{TDG} within the well water column prior to pumping (i.e., degassed water) as an empty square at $t = 20$ days. Water pressure measurements are shown as black circles. (B) Close-up of the first 24 h (indicated by the red rectangle in Figure 4A), showing the approximate interval where the key mechanism controlling in-well degassing transitioned from advective and bubble-driven convection to thermal driven convection (shown as a vertical dashed line). The colors have the same meaning in A and B.

Gas Species Composition Profiles

The dominant in situ gas species in "fresh" groundwater (CH_4, N_2, and CO_2) dominated in the vertical gas composition profile obtained from gas samples collected using PGD samplers during the pre- and post-pumping sampling (Figure 5). On average, gas composition in the pre-pumping gas samples were 77.9% CH_4, 21.5% N_2, 0.2% CO_2, 0.3% O_2, 0.1% Ar, and non-detectable SF_6 (Table S2; Figure 5A). The increased contribution of N_2, O_2, and Ar in pre-pumping gas samples provides evidence that mixing with atmospheric gases had occurred in the SWC (Figure 5A. While Ar was detected at all depths, O_2 was detected only at 3.5, 22.5, and 36.5 m bswl. In particular, the presence of detectable O_2 in all of the samples collected during the pre-pumping monitoring interval suggests interaction with the atmosphere. The possibility of atmospheric contamination during sample collection and analysis is discussed below.

Post-pumping composition profiles of gas samples collected using PGD samplers remained relatively constant with depth, with an average gas composition of 92.5% CH_4, 6.8% N_2, 0.2% CO_2, 0.0% O_2, 0.0% Ar, and 0.5% SF_6 (Table S2; Figure 5B). Contrary to the pre-pumping period, O_2 and Ar were not detected in any of the samples collected in the post-pumping monitoring period (Figure 5B), indicating that the presence of SF_6 in the well's casing headspace restricted interaction with the atmosphere.

The detection of SF_6 was all monitoring depths in gas samples collected using PGD samplers suggests substantial mixing in the well column occurred during the 15-day monitoring period. As SF_6 has a small diffusion coefficient ($\sim 0.78 \times 10^{-9}$ m^2 s^{-1} at 7°C; King and Saltzman 1995), SF_6 that was bubbled into the top of the water column could not be transported several meters within the water column by diffusion alone (which is estimated to occur at a rate of approximately 0.01 m/day; Appendix S1). The lack of Ar and O_2 detection in any of the post-pumping samples is consistent with "fresh" groundwater gases and mixing with SF_6 from the well casing headspace, and indicates that atmospheric contamination during sampling or analysis did not occur in these samples. Given identical sampling, storage, and analytical procedures for both sampling campaigns, it is unlikely atmospheric contamination occurred in the pre-pumping samples.

Estimated Gas Concentration Profiles

Despite the relatively similar volumetric gas composition with depth during both sampling campaigns, estimated dissolved CH_4 concentration increased significantly with depth as a function of increased P_{TDG} (Equations 4 and 5; Figure 6). Pre-pumping gas samples were collected when the well water column was substantially degassed, while post-pumping samples were collected when degassing was still actively occurring and P_{TDG} was elevated (as discussed above). The consequently higher P_{TDG} values observed during the post-pumping period are reflected in higher estimated dissolved gas concentrations (Figure 6).

Since P_{TDG} during the pre-pumping period was lower at all monitoring depths, pre-pumping estimated CH_4 and CO_2 concentrations were also significantly lower than the 15-days post-pumping estimated concentrations (Figure 6A and 6D). However, the same pattern was not observed for the major atmospheric gases (N_2, O_2, and Ar), which were higher during the pre-pumping sampling (Figure 6B, 6C, and 6E). While estimated O_2 concentrations decreased with depth during the pre-pumping sampling (Figure 6C), estimated CH_4 concentrations increased with depth during both sampling campaigns (Figure 6A). Finally, estimated N_2, CO_2, Ar, and SF_6 concentrations did not show any consistent trend with depth (Figure 6B, Figure 6D, Figure 6E, and Figure 6F).

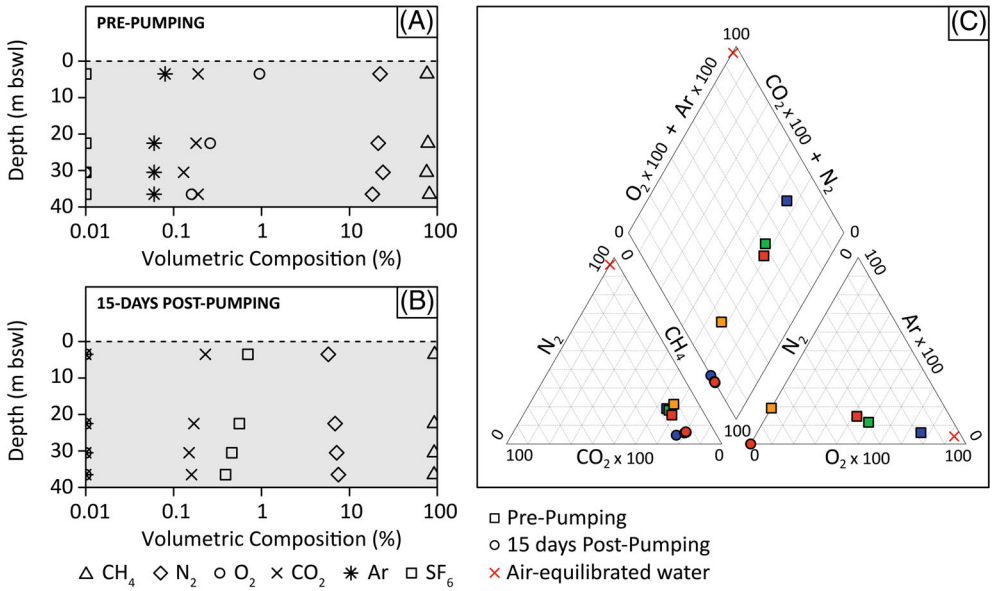

Figure 5. Average vertical volumetric gas composition profiles of CH_4, N_2, CO_2, SF_6, O_2, and Ar as measured in passive gas diffusion samples (A) prior to pumping and (B) 15 days post-pumping. Non-detectable concentrations are plotted as 0.01%. (C) Depth-averaged volumetric gas composition prior to pumping (squares), 15 days post-pumping (circles), and for air-equilibrated water. The symbol colors correspond to sampling depths (c.f. Figure 1).

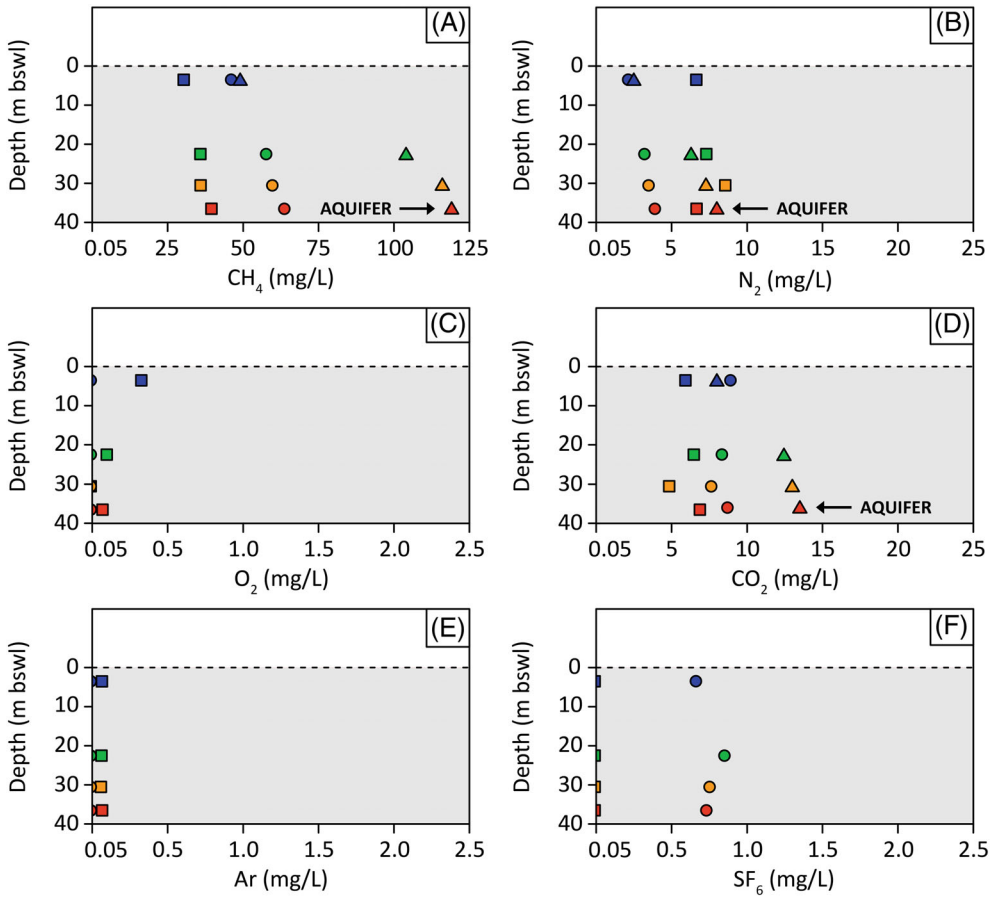

Figure 6. Estimated vertical concentration profiles (mg/L) of major gas species (CH_4, N_2, CO_2, SF_6, O_2, and Ar) pre- (□), 6-h post- (Δ) and 15-days post- (○) pumping. Estimated aquifer CH_4, N_2, CO_2 concentrations based on post-pumping gas composition and max P_{TDG} measured at the deepest monitoring depth (36.5 m bswl) are indicated by the black arrow. Non-detectable concentrations are plotted as 0.05 mg/L.

Pre- and 15 days post-pumping estimated groundwater gas concentrations with depth within the well water column provided additional evidence of in-well mixing and degassing. As estimated dissolved gas concentrations reflected the measured P_{TDG} at the time of sample collection, our findings confirmed previous studies that gas-charged groundwater wells become degassed after pumping (Roy and Ryan 2010; Banks et al. 2017; Evans 2017). In this study, increasing estimated CH_4 and N_2 gas concentrations with depth demonstrated that the degassing was still actively happening in the SWC 15 days after pumping ceased (Figures 2 and 4).

Finally, while P_{TDG} corrected CH_4 concentrations were significantly different depending on where and when P_{TDG} measurements were collected. For example, at the deepest monitoring point (36.5 m bswl), the estimated CH_4 concentrations at the end of the post-pumping monitoring period (i.e., 63.5 mg/L) was about half that estimated when the maximum P_{TDG} was measured (i.e., 6 h post-pumping; 119.3 mg/L; Figure 6). Therefore, findings from this study confirmed that long-term in situ P_{TDG} monitoring during sampling is useful to accurately estimate in situ dissolved gas concentrations (Ryan et al. 2015).

In-Well Mixing and Degassing Mechanism

After a significant rise in P_{TDG} during and shortly after "fresh" groundwater was pumped into the well, P_{TDG} values decreased at all depths throughout the post-pumping period, indicating the occurrence of in-well degassing (Figure 4). As previously discussed, bubble formation and consequent degassing is only expected to occur at depths where $P_{TDG} \approx P_{BUB}$. However, P_{TDG} values consistently decreased to below the corresponding P_{BUB} at the three deeper monitoring depths within the SWC, including at the deepest depth where the P_{BUB} substantially exceeded the in situ aquifer P_{TDG} (Table 2; Figures 2 and 3E–3H). This implies that, although bubble formation is important in the early post-pumping period, additional mechanisms, like well water flow and thermal gradients must contribute to in-well mixing. Additional evidence of in-well mixing was provided by gas compositional analysis. The similar compositional proportion of CH_4 relative to other gas species with depth observed during both monitoring periods is consistent with mixing of gases from "fresh" aquifer water upwards within the entire SWC, and atmospheric (and tracer) gas species downwards.

As the recovery to static water level occurred several hours after pump shut off, favorable conditions for the occurrence of hydrostatic gradient driven convection were observed for the first 16 h of the post-pumping monitoring period. In agreement with previous studies that have demonstrated the occurrence of significant mixing in groundwater wells and vertical water columns due to the occurrence of hydraulic gradient and bubble-driven convective flows (Barczewski et al. 1993; Berthold and Börner 2008; Berthold 2010; Almeras et al. 2015), results from this study imply that fresh groundwater entering the well screen with elevated P_{TDG} formed bubbles whose buoyant migration induced significant mixing within the well water column by upward bubble migration-induced flow and turbulence. The occurrence of hydraulic gradient and bubble-driven convection resulted in the movement of deeper water (with higher P_{TDG}) upwards in the well water column, where lower P_{BUB} values permitted degassing until $P_{TDG} \approx P_{BUB}$ and, at the same time, reinforced the occurrence of short-term in-well mixing and degassing. Additional evidence of hydraulic gradient and bubble-driven mixing was provided by the higher rates of degassing shortly after pumping (16 h; Figure 4B) at monitoring depths where $P_{TDG} \approx P_{BUB}$.

However, despite P_{TDG} being close to saturation (P_{BUB}) only for the first approximately 16 h at 22.5 and 30.5 m bswl, degassing was still occurring at all monitoring depths 15 days after pumping ceased (Figures 2 and 4). This suggests that processes other than the formation of FPG and hydraulic gradient driven convection were inducing the occurrence of long-term mixing and degassing.

As previously discussed, in-well mixing can also occur due to the existence of a significant thermal gradient within the well water column. Water temperature measurements from the minisondes installed at 3.5 and 30.5 m bswl indicated an average thermal gradient of 0.017C°/m over both monitoring periods (Appendix S1; Table S1). Despite some minor fluctuations, the thermal gradient between the two monitoring points remained relatively constant over the entire monitoring period (Appendix S1 and Figure S2), indicating that the observed values were likely associated with the in situ temperature gradient in the SWC. Previous studies have demonstrated that the occurrence of thermally induced convection currents in vertical water columns at a normal in situ gradient (Solodov et al. 2002; Berthold and Börner 2008).

All parameters used in our calculations are shown in Table 3. While calculations from Equation 6 indicated an average thermal Rayleigh number of approximately 298, the substitution of values in Equation 7 indicated a critical thermal Rayleigh number of approximately 147 (Figure 7). As Ra_T is greater than Ra_{TC}, we can conclude that the development of thermal convection was expected to occur over the entire monitoring period.

Therefore, findings from this study demonstrated that the occurrence of hydraulic gradient and bubble-driven convection were keys mechanisms controlling the short term (i.e., first 16 h) in-well mixing and degassing observed, while thermal gradient-induced mixing was expected to consistently occur in the well. The sum of these three mechanisms resulted in gas species mixing within the entire SWC, including the depths where P_{TDG} was lower than the corresponding P_{BUB}. Although the relative contribution and degree of each mechanism is well dependent (e.g., aquifer P_{TDG}, P_{BUB} at the screened interval, and the regional thermal gradient), findings from this study confirmed that in-well mixing is a key process controlling degassing in gas-charged groundwater wells.

Table 3
Physical Parameter Values Used in Equations 6 and 7 for Stability Analyses to Evaluate Thermally Driven Convection in the Well Water Column

Parameter	Value
Gravity acceleration	$9.81\ m\ s^{-2}$
Thermal expansion coefficient	$4.47 \times 10^{-5}\ K^{-1}$ (after Chen and Millero 1986)
Average temperature at 3.5 m bswl	279.93 K
Average temperature at 30.5 m bswl	280.38 K
Radius of the water column	0.055 m
Height of the water column	40.50 m
Kinematic viscosity of water	$1.40 \times 10^{-6}\ m^2\ s^{-1}$ (after Pritchard 2011)
Thermal diffusivity of water	$1.36 \times 10^{-7}\ m^2\ s^{-1}$ (after James 1968)
Thermal conductivity of water	$0.60 \times 10^{-6}\ W\ K^{-1}\ m^{-1}$ (after Dixon 2007)
Thermal conductivity of the surrounding geologic formations	$2.10 \times 10\ W\ K^{-1}\ m^{-1}$ (after Robertson 1988)

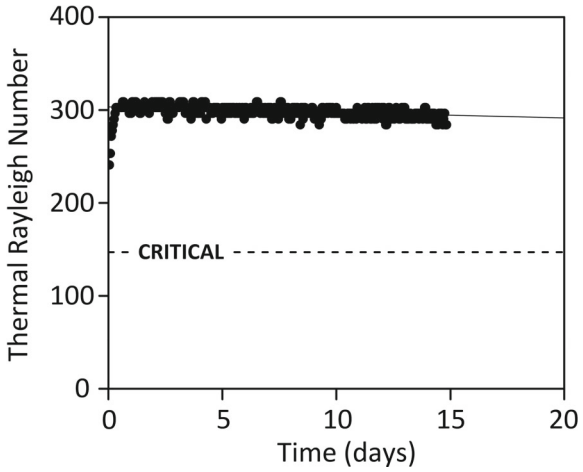

Figure 7. Time series of calculated thermal Rayleigh numbers based on the temperature gradient measured by the minisondes deployed at 3.5 and 30.5 m bswl during the post-pumping monitoring period. The value for the critical thermal Rayleigh number is shown as a black dashed line.

Conclusions

Multiple lines of evidence indicated that active in-well degassing occurred after groundwater was pumped from a gas-charged groundwater well. Pre-pumping P_{TDG} monitoring at four deployment depths (up to 36.5 m bswl) in the groundwater monitoring well showed P_{TDG} values that were substantially below P_{BUB} at the three deeper monitoring depths (22.5, 30.5, and 36.5 m bswl). In addition, vertical P_{TDG} profiles indicated that ongoing loss of groundwater gases was actively occurring even more than 15 days after the well was last pumped.

The P_{TDG} increased during and immediately after pumping, with maximum values that were consistent with the expected vertical distribution of P_{TDG} in the absence of in-well mixing and degassing (i.e., $P_{TDG} \approx P_{BUB}$ until P_{BUB} reaches the in situ aquifer P_{TDG} at ~31.0 m bswl). The maximum P_{TDG} values were observed about 6 h after pumping was ceased, while the water level in the well was still recovering (i.e., P_{BUB} was continuing to increase), but before in-well mixing caused substantial degassing to occur.

Dissolved gas composition analyses confirmed that significant in-well mixing occurred over the entire well water column in both directions (i.e., the dominant groundwater gas (CH_4) was mixed upwards and atmospheric O_2 and a shallow tracer (SF_6) introduced after pumping were mixed downwards). Additional evidence of in-well mixing was provided by a continual decline in P_{TDG} over the 15-day post-pumping monitoring period.

Monitoring of vertical P_{TDG} with depth demonstrated that the formation of bubbles and the occurrence of hydraulic gradient and bubble-driven convection are key mechanisms controlling degassing in gas-charged wells during and shortly after pumping (i.e., in the first 16 h of water level recovery), including at depths where P_{TDG} is lower than P_{BUB}. In addition, the measurement of similar gas composition and significant temperature gradients with depth over the entire monitoring period indicated that long-term thermally driven convention can potentially be a key mechanism controlling long-term degassing in groundwater wells with substantial thermal gradient.

As the occurrence of vertical convection can result in mixing (i.e., degassing) throughout the entire water column, long-term monitoring of P_{TDG} at the screened interval will require pumping and/or the use of packers to be representative of in situ aquifer P_{TDG}. Furthermore, mixing within the wellbore water column can induce significant mass exchange between the well and aquifer water, increasing the amount of water that should be pumped prior to sampling. Findings from this study have provided insight into the degassing mechanisms and conditions within an over-pressured groundwater well after pumping.

Acknowledgments

This study was funded by the Canada First Research Excellence (CFREF) Fund's "Global Research Initiative in Sustainable Low Carbon Unconventional Resources" and Natural Science and Engineering Research Council

(NSERC). We give thanks to Alberta Environment and Parks (AEP) for providing access to their well.

Conflict of Interest

The authors do not have any conflicts of interest to report.

Supporting Information

Additional supporting information may be found online in the Supporting Information section at the end of the article. Supporting Information is generally *not* peer reviewed.

Appendix S1 Supporting Information (It may be found online in the Supporting Information section at the end of the article and includes additional table and figures, including a time-series figure of the temperature measurements, a figure of the recovery after well pumping, a table of the average temperature and dissolved O_2 measured by the hydrolabs, and a table of the average gas composition measured. Addition information regarding the voltage corrections for P_{TDG} readings and the downhole transport of SF_6 through diffusion is also provided. The supporting information was not subjected to peer-review).

References

Almeras, E., F. Risso, V. Roig, S. Cazin, C. Plais, and F. Augier. 2015. Mixing by bubble-induced turbulence. *Journal of Fluid Mechanics* 776, no. 1: 458–474.

Amos, R.T., K.U. Mayer, B.A. Bekins, G.N. Delin, and R.L. Williams. 2005. Use of dissolved and vapor-phase gases to investigate methanogenic degradation of petroleum hydrocarbon contamination in the subsurface. *Water Resources Research* 41, no. 2: 1–15.

Banks, E.W., S.D. Smith, M. Hatch, L. Burk, and A. Suckow. 2017. Sampling dissolved gases in groundwater at in situ pressure: A simple method for reducing uncertainty in hydrogeological studies of coal seam gas exploration. *Environmental Science & Technology Letters* 4, no. 12: 535–539.

Barczewski, B., J. Grimm-Strehle, and G. Bisch. 1993. Suitability test of groundwater monitoring wells. *WasserWirtschaft* 83, no. 1: 72–78.

Berthold, S., and F. Börner. 2008. Detection of free vertical convection and double-diffusion in groundwater monitoring wells with geophysical borehole measurements. *Environmental Geology* 54, no. 7: 1547–1566.

Berthold, S. 2010. Synthetic convection log: Characterization of vertical transport processes in fluid-filled boreholes. *Journal of Applied Geophysics* 72, no. 1: 20–27.

Blicher-Mathiesen, G., G.W. McCarty, and L.P. Nielsen. 1998. Denitrification and degassing in groundwater estimated from dissolved dinitrogen and argon. *Journal of Hydrology* 208, no. 1-2/2: 16–24.

Blyth, A., and A. Mellor. 2009. Rosebud and Redland monitoring well installation report. Alberta Environment Open-File Report.

Boot-Handford, M.E., J.C. Abanades, E.J. Anthony, M.J. Blunt, S. Brandani, N. Mac Dowell, J.R. Fernandez, M.C. Ferrari, R. Gross, J.P. Hallett, R.S. Haszeldine, P. Heptonstall, A. Lyngfelt, Z. Makuch, E. Mangano, R.T.J. Porter, M. Pourkashanian, G.T. Rochelle, N. Shah, J.G. Yao, and P.S. Fennell. 2014. Carbon capture and storage update. *Energy & Environmental Science* 7, no. 1: 130–189.

Bordeleau, G., C. Rivard, D. Lavoie, and R. Lefebvre. 2021. A systematic multi-isotope approach to unravel methane origin in groundwater: Example of an aquifer above a gas field in southern New Brunswick (Canada). *Applied Geochemistry* 134: 105077.

Busenberg, E., and L.N. Plummer. 2010. A rapid method for the measurement of sulfur hexafluoride (SF6), trifluoromethyl sulfur pentafluoride (SF5CF3), and Halon 1211 (CF2ClBr) in hydrologic tracer studies. *Geochemistry, Geophysics, Geosystems*, 11, no. 11: 1–10.

Cahill, A.G., C.M. Steelman, O. Forde, O. Kuloyo, S. Emil Ruff, B. Mayer, K.U. Mayer, M. Strous, M.C. Ryan, J.A. Cherry, and B.L. Parker. 2017. Mobility and persistence of methane in groundwater in a controlled-release field experiment. *Nature Geoscience* 10, no. 4: 289–294.

Campbell, A.E., L.K. Lautz, and G.D. Hoke. 2022. Temporal changes in domestic water well methane reflects shifting sources of groundwater: Implications for evaluating contamination attributed to shale gas development. *Applied Geochemistry* 166: 105175.

Castellon, L. 2009. *Dissolved gas measurements in Alberta groundwater monitoring wells*. Unpublished MSc Capstone Project, University of Calgary.

Chen, C.-T. A., and Millero, F. J. 1986. Thermodynamic properties for natural waters covering only the limnological range. *Limnology and Oceanography* 31, no. 3: 657–662.

Clark, J.F., G.B. Hudson, M.L. Davisson, G. Woodside, and R. Herndon. 2004. Geochemical imaging of flow near an artificial recharge facility, Orange County, California. *Groundwater* 42, no. 2: 167–174.

Climent, E., and J. Magnaudet. 1999. Large-scale simulations of bubble-induced convection in a liquid layer. *Physical Review Letters* 82, no. 24: 4827–4830.

D'Aoust, B.G. 2007. Technical note: Total dissolved gas pressure (TDGP) sensing in the laboratory. *Dissolution Technologies* 14, no. 2: 38–41.

Dixon, J. C. 2007. *The Shock Absorber Handbook*, 2nd ed. Hoboken, NJ: John Wiley & Sons.

Evans, R. 2017. Towards accurate in situ dissolved gas concentration estimations in gas-charged groundwater using field measured total dissolved gas pressure (PTDG). Unpublished MSc thesis, University of Calgary.

Forde, O.N., A.G. Cahill, K.U. Mayer, B. Mayer, R.L. Simister, N. Finke, S.A. Crowe, J.A. Cherry, and B.L. Parker. 2019. Hydro-biogeochemical impacts of fugitive methane on a shallow unconfined aquifer. *Science of the Total Environment* 690: 1342–1354.

Gershuni, G.Z., and E.M. Zhukhovitskii. 1976. *Convective Stability of Incompressible Fluids*. Jerusalem, Israel: Keter Publishing House.

Hammond, P.A. 2016. The relationship between methane migration and shale-gas well operations near Dimock, Pennsylvania, USA. *Hydrogeology Journal* 24, no. 2: 503–519.

Harden, H.S., J.P. Chanton, J.B. Rose, D.E. John, and M.E. Hooks. 2003. Comparison of sulfur hexafluoride, fluorescein and rhodamine dyes and the bacteriophage PRD-1 in tracing subsurface flow. *Journal of Hydrology* 277, no. 1-2: 100–115.

Humez, P., B. Mayer, J. Ing, M. Nightingale, V. Becker, A. Kingston, O. Akbilgic, and S. Taylor. 2016. Occurrence and origin of methane in groundwater in Alberta (Canada): Gas geochemical and isotopic approaches. *Science of the Total Environment* 541: 1253–1268.

Jackson, R.E., A.W. Gorody, B. Mayer, J.W. Roy, M.C. Ryan, and D.R. Van Stempvoort. 2013. Groundwater protection and unconventional gas extraction: The critical need for field-based hydrogeological research. *Groundwater* 51, no. 4: 488–510.

James, D.W. 1968. The thermal diffusivity of ice and water between- 40 and + 60 C. *Journal of Materials Science* 3, no. 5: 540–543.

Kelly, W.R., G. Matisoff, and J.B. Fisher. 1985. The effects of a gas well blow out on groundwater chemistry. *Environmental Geology and Water Sciences* 7, no. 4: 205–213.

King, D.B., and E.S. Saltzman. 1995. Measurement of the diffusion coefficient of sulfur hexafluoride in water. *Journal of Geophysical Research* 100, no. C4: 7083–7088.

Li, Y., N.A. Thelemaque, H.G. Siegel, C.J. Clark, E.C. Ryan, R.J. Brenneis, K.M. Gutchess, M.A. Soriano Jr., B. Xiong, N.C. Deziel, J.E. Saiers, and D.L. Plata. 2021. Thermogenic sources and hydrogeomorphology migration pathways. *Environmental Science and Technology* 55: 16413–16422.

Lindeberg, E., P. Bergmo, M. Torsr, and A.-A. Grimstad. 2017. Aliso canyon leakage as an analogue for worst case CO_2 leakage and quantification of acceptable storage loss. *Energy Procedia* 114: 4279–4286.

Love, A.J., C.T. Simmons, and D.A. Nield. 2007. Double-diffusive convection in groundwater wells. *Water Resources Research* 43: W08428.

Lu, X., A. Watson, A.V. Gorin, and J. Deans. 2005. Measurements in a low temperature CO2-driven geysering well, viewed in relation to natural geysers. *Geothermics* 34, no. 4: 389–410.

Manning, A.H., D.K. Solomon, and A.L. Sheldon. 2003. Applications of a total dissolved gas pressure probe in groundwater studies. *Groundwater* 41, no. 4: 440–448.

McLeish, K., M.C. Ryan, and A. Chu. 2007. Integrated sampling and analytical approach for common groundwater dissolved gases. *Environmental Science and Technology* 41, no. 24: 8388–8393.

Pritchard, P.J. 2011. *Fox and McDonald's Introduction to Fluid Mechanics*. 8th ed. New York, NY: John Wiley & Sons.

Rayleigh, L. 1916. On convection currents in a horizontal layer of fluid, when the higher temperature is on the under side. *Philosophical Magazine* 6, no. 32: 529–546.

Robertson, E.C. 1988. Thermal properties of rocks. USGS Open File Report 88–441.

Roy, J.W., G. Bordeleau, C. Rivard, M.C. Ryan, X. Malet, S.J. Brown, and V. Tremblay. 2022. Continual long-term monitoring of methane in wells above the Utica shale using total dissolved gas pressure probes. *Hydrogeology Journal* 30: 1005–1019. https://doi.org/10.1007/s10040-022-02452-1

Roy, J.W., and M.C. Ryan. 2013. Effects of unconventional gas development on groundwater: A call for total dissolved gas pressure field measurements. *Groundwater* 51, no. 4: 480–482.

Roy, J.W., and M.C. Ryan. 2010. In-well degassing issues for measurements of dissolved gases in groundwater. *Groundwater* 48, no. 6: 869–877.

Ryan, M.C., J.W. Roy, and D.J. Heagle. 2015. Dissolved gas 'concentrations' or 'concentration estimates'—A comment on "Origin, distribution and hydrogeochemical controls on methane occurrences in shallow aquifers, southwestern Ontario, Canada". by Jennifer C. McIntosh, Stephen E. Grasby, Stewart M. Hamilton, and Stephen G. Osborn, *Applied Geochemistry*. 63: 218–221.

Ryan, M.C., K.T.B. MacQuarrie, J. Harman, and J. McLellan. 2000. Field and modeling evidence for a "stagnant flow" zone in the upper meter of sandy phreatic aquifers. *Journal of Hydrology* 233, no. 1-4: 223–240.

Sander, R. 2015. Compilation of Henry's law constants (version 4.0) for water as solvent. *Atmospheric Chemistry and Physics* 15: 4399–4981.

Sanford, W.E., R.G. Shropshire, and D.K. Solomon. 1996. Dissolved gas tracers in groundwater: Simplified injection, sampling, and analysis. *Water Resources Research* 32, no. 6: 1635–1642.

Solodov, I.N., V.I. Malkovsky, A.A. Pek, and S.M. Benson. 2002. New evidence for the combined influence of vapor condensation and thermal convection on groundwater monitoring wells. *Environmental Geology* 42, no. 2-3: 145–150.

Solomon, D.K., E. Cole, and J.F. Leising. 2011. Excess air during aquifer storage and recovery in an arid basin (Las Vegas Valley, USA). *Hydrogeology Journal* 19, no. 1: 187–194.

Spalding, B.P., and D.B. Watson. 2008. Passive sampling and analysis of common dissolved fixed gases in groundwater. *Environmental Science and Technology* 42, no. 10: 3766–3772.

Spalding, B.P., and D.B. Watson. 2006. Measurement of dissolved H_2, O_2, and CO_2 in groundwater using passive samplers for gas chromatographic analyses. *Environmental Science and Technology* 40, no. 24: 7861–7867.

Vengosh, A., R.B. Jackson, N. Warner, T.H. Darrah, and A. Kondash. 2014. A critical review of the risks to water resources from unconventional shale gas development and hydraulic fracturing in the United States. *Environmental Science and Technology* 48, no. 15: 8334–8348.

Waddington, J.M., S.J. Ketcheson, E. Kellner, M. Strack, and A.J. Baird. 2009. Evidence that piezometers vent gas from peat soils and implications for pore-water pressure and hydraulic conductivity measurements. *Hydrological Processes* 23, no. 8: 1249–1254.

Watson, Z.T., W.S. Han, E.H. Keating, N.H. Jung, and M. Lu. 2014. Eruption dynamics of CO_2-driven cold-water geysers: Crystal, Tenmile geysers in Utah and Chimayó geyser in New Mexico. *Earth and Planetary Science Letters* 408: 272–284.

Watson, A.J., J.R. Ledwell, and S.C. Sutherland. 1991. The Santa Monica Basin tracer experiment: Comparison of release methods and performance of perflurodecalin and sulfur hexafluoride. *Journal of Geophysical Research* 96, no. C5: 8719–8725.

Wilson, R.D., and D.M. Mackay. 1995. Direct detection of residual nonaqueous phase liquid in the saturated zone using SF6 as a partitioning tracer. *Environmental Science and Technology* 29, no. 5: 1255–1258.

Wilson, R.D., and D.M. Mackay. 1993. The use of sulfur hexafluoride as a conservative tracer in saturated sandy media. *Groundwater* 31, no. 5: 719–724.